HHS Public Access

Author manuscript

Mol Cell Endocrinol. Author manuscript; available in PMC 2018 January 30.

Published in final edited form as:

Mol Cell Endocrinol. 2016 November 15; 436: 41–49. doi:10.1016/j.mce.2016.07.009.

Quantitative Proteomic Profiling Reveals Hepatic Lipogenesis and Liver X Receptor Activation in the PANDER Transgenic Model

Mark G. Athanason, **Whitney A. Ratliff**, **Dale Chaput**, **Catherine B. MarElia**, **Melanie N. Kuehl**, **Stanley M. Stevens Jr.**, and **Brant R. Burkhardt***

Department of Cell Biology, Microbiology and Molecular Biology, University of South Florida, 4202 East Fowler Avenue, Tampa, FL 33620

Abstract

PANcreatic-DERived factor (PANDER) is a member of a superfamily of FAM3 proteins modulating glycemic levels by metabolic regulation of the liver and pancreas. The precise PANDER-induced hepatic signaling mechanism is still being elucidated and has been very complex due to the pleiotropic nature of this novel hormone. Our PANDER transgenic (PANTG) mouse displays a selective hepatic insulin resistant (SHIR) phenotype whereby insulin signaling is blunted yet lipogenesis is increased, a phenomena observed in type 2 diabetes. To examine the complex PANDER-induced mechanism of SHIR, we utilized quantitative mass spectrometry based proteomic analysis using Stable Isotope Labeling by Amino Acids in Cell Culture (SILAC) to reveal the global hepatic proteome differences within the PANTG under the metabolic states of fasting, fed and insulin-stimulated conditions. Proteomic analysis identified lipid metabolism as one of the top cellular functions differentially altered in all metabolic states. Differentially expressed proteins within the PANTG having a lipid metabolic role included ACC, ACLY, CD36, CYP7A1, FASN and SCD1. Central to the differentially expressed proteins involved in lipid metabolism was the predicted activation of the liver X receptor (LXR) pathway. Western analysis validated the increased hepatic expression of LXRα along with LXR-directed targets such as FASN and CYP7A1 within the PANTG liver. Furthermore, recombinant PANDER was capable of inducing LXR promoter activity *in-vitro* as determined by luciferase reporter assays. Taken together, PANDER strongly impacts hepatic lipid metabolism across metabolic states and may induce a SHIR phenotype via the LXR pathway

Keywords

Fam3B; PANDER; liver; lipogenesis; fatty acid synthesis; Liver X Receptor; SILAC; proteomics

*Corresponding Author: Brant R. Burkhardt, Ph.D., Department of Cell Biology, Microbiology and Molecular Biology, University of South Florida, 4202 East Fowler Avenue, BSF 206, Tampa, FL 33620, Tel: 813-974-5968, Fax: 813-974-1644, bburkhardt@usf.edu.

1. INTRODUCTION

Over the past decade PANcreatic-DERived factor (PANDER or FAM3B) has been investigated with regard to secretion from the endocrine pancreas and biological impact on glycemic regulation both *in-vitro* and *in-vivo* (Zhu, Xu, Patel et al., 2002, Burkhardt, Cook, Young et al., 2008, Burkhardt, Greene, White et al., 2006, Cao, Yang, Burkhardt et al., 2005, Hou, Wang, Li et al., 2011, Mou, Li, Yao et al., 2013, Robert, 2005, Robert-Cooperman, Carnegie, Wilson et al., 2010, Wang, Cai, Pang et al., 2008, Xiang, Chen and Yang, 2012, Xu, Gao, Wu et al., 2005, Yang, Gao, Robert et al., 2005, Yang, Robert, Burkhardt et al., 2005, Zhuang, Guan, Gao et al., 2011). Our recently generated pancreas specific overexpressing transgenic mouse model (PANTG) exhibits both fasting and fed glucose intolerance primarily attributed to impaired hepatic insulin signaling concordantly coupled with both increased gluconeogenesis and lipogenesis (Robert-Cooperman, Dougan, Moak et al., 2014). This result is consistent with other PANDER animal models that acutely express PANDER within the liver via adenoviral delivery (Li, Chi, Wang et al., 2011). The mechanism by which PANDER inhibits hepatic insulin signaling has been attributed to suppressed phosphorylation of Akt (Yang, Wang, Li et al., 2009) and AMPK (Robert-Cooperman et al., 2014). Both of which serve as major regulators of gluconeogenesis. However, a major paradox to PANDER signaling has been the documented increase in hepatic lipogenesis despite inhibited insulin signaling (Robert-Cooperman et al., 2014, Li et al., 2011). This bifurcation of signaling results in a selective insulin resistant state that mimics what is observed in T2D animal models and humans (Biddinger, Hernandez-Ono, Rask-Madsen et al., 2008, Brown and Goldstein, 2008). Encompassing prior PANDER research, an emerging hypothesis suggests that the pathophysiological conditions of T2D could potentially induce increased circulating PANDER levels contributing to selective hepatic insulin resistance (SHIR) resulting in increased hepatic glucose output and lipogenesis (Wilson, Robert-Cooperman and Burkhardt, 2011, Wang, Burkhardt, Guan et al., 2012), as precisely observed in our PANTG model. Recent evidence has now indicated that circulating PANDER levels are elevated and associated with metabolic syndrome components in a Chinese population (Cao, Yang, Lai et al., 2015). Plasma PANDER levels significantly correlated with fasting plasma glucose, 2 hour plasma glucose, and triglyceride levels. Between animal model results and recent clinical studies, an emerging theme with PANDER is the possible role of this novel hormone in the promotion of hepatic insulin resistance and lipogenesis. Despite this importance, the precise PANDER-induced signaling mechanism in the liver has yet to be determined.

To elucidate PANDER-induced hepatic molecular mechanisms, we utilized quantitative mass spectrometry-based proteomic analysis via a stable isotope labeling by amino acids in cell culture (SILAC) approach to characterize hepatic proteomic differences between the PANTG murine liver with that of wild-type mice under three metabolic states: fasting, fed, and insulin-stimulated. To achieve this, stable isotope-labeled liver protein lysate from mice that were metabolically labeled with $^{13}C_6$-Lys was utilized as an internal standard for relative quantification of global proteome differences in the liver, a technique rarely used to study metabolic disorders yet previously validated from examination of insulin signaling and liver proteomic characterization. Differentially expressed proteins using this approach can be

analyzed with bioinformatics tools such as Ingenuity Pathway Analysis (IPA) in order to reveal altered molecular networks and their function as well as differences in canonical pathways that can be later validated via additional molecular approaches. This unbiased, global-scale approach has led to novel insight into PANDER-induced hepatic pathway alterations in our PANTG model, in particular, those related to increased lipogenesis.

2. MATERIALS AND METHODS

2.1. Transgenic mouse generation and genotyping

Generation and original phenotyping of the PANDER transgenic mouse was described previously (Robert-Cooperman et al., 2014). In brief, this murine model overexpresses PANDER from the endocrine pancreas resulting in increased levels of circulating PANDER with a phenotype of impaired glucose tolerance and hepatic insulin sensitivity.

2.2. Proteomic Experimental Design

The purpose of this study was to examine the PANDER-induced hepatic proteome in various metabolic states. As outlined in Fig. 1, the PANTG mouse was exposed to fasted, fed, and insulin stimulatory conditions prior to liver extraction and subsequent proteomic examination. All treatments were performed on PANTG and wild-type mice at six weeks of age. Fed and fasted mice were withheld from food for approximately 4 and 16 hours, respectively. Following the 4 hour fast, fed mice were provided with chow *ad-libitum* for 2 hours. Insulin-stimulated mice were fasted for 4 hours prior to insulin injection (Humulin®, 1 unit/kg). Insulin was diluted to 20 units/ml and injected intraperitoneally with exposure for 15 minutes. Mice were humanely euthanized by carbon dioxide asphyxiation and cervical dislocation following above described metabolic conditions. Livers were extracted immediately following exposure to described metabolic conditions, snap frozen and stored at −80°C prior to proteomic analysis.

2.3. Hepatic Protein Isolation

Approximately 40 mg of tissue was excised from a lobe of mouse liver for tissue lysis. Tissue was submerged in cold lysis buffer (100mM Tris-HCl, 100mM DTT, 4% SDS and 1x HALT protease inhibitor) and homogenized using a Qiagen TissueRupter. Cell lysate was then heated at 95°C for five minutes followed by brief sonication. The tissue lysate was cleared by centrifugation at 16000× *g* for 5 min and the supernatant was collected and stored at −80°C prior to further analysis. The same procedure for protein purification was performed on the “heavy” labeled ($^{13}C_6$ L-Lysine) murine male liver (MT-LYSC6-ML-PK, Cambridge Isotope Laboratories, Inc.).

2.4. Sample digestion, desalt and SCX fractionation

Protein concentration was quantified using the Pierce 660 nm protein assay kit supplemented with the provided ionic detergent compatibility reagent (IDCR). Equal mass of labeled and unlabeled protein or “light” and “heavy” protein respectively, were combined and digested using the filter-aided sample preparation (FASP) method (Expedeon). Briefly, 30 μL of the protein mixture (~12.5mg/ml) was added to the spin column. The lysate buffer was exchanged to 8M urea using centrifugation prior to alkylation by iodoacetamide. The

solution was then exchanged to 50 mM ammonium bicarbonate for trypsin/Lys-C digestion at a ratio of 1:40 (w/w). Digestion was carried out overnight in a humidified incubator at 37°C. Peptides were eluted off the column by addition of 0.5M NaCl followed by centrifugation.

Samples were desalted using solid phase enrichment C18 columns (The Nest Group, Inc.). Briefly, columns were activated using 100% acetonitrile followed by equilibration with 0.1% formic acid in water. Samples were loaded onto the columns and washed three times using equal volumes of 0.1% formic acid in water. Samples were eluted using 90% acetonitrile/ 0.1% formic acid in water and then concentrated in a vacuum concentrator (Thermo) prior to resuspension with 5 mM ammonium formate and 25% acetonitrile. Peptides were fractionated by strong cation exchange chromatography as previously described (Bell-Temin, Culver-Cochran, Chaput et al., 2015).

2.5. LC-MS/MS and pathway analysis

Fractions were separated on a 10 cm × 75 μm I.D. reversed phase column packed with 5 μm C18 material with 300 Å pore size (New Objective) using 120 minute gradients of 2–40% ACN in 0.1% formic acid. Inline mass spectrometric analysis was performed on a hydrid linear ion trap-Orbitrap mass spectrometer (Orbitrap XL (Thermo Fisher Scientific). Full MS survey scans were performed at a resolving power of 60000, and the top 10 most abundant peaks were selected for subsequent MS/MS analysis in the linear ion trap. Raw files were processed in MaxQuant 1.2.2.5 employing the Andromeda search algorithm and searched against the UniprotKB reference database for *Mus musculus*, concatenated with reversed protein sequences. A second database of known contaminants provided with the MaxQuant suite was also employed. All fractions for each biological sample were combined for analysis. Constant modification of carbamidomethylation of cysteine and variable modifications of oxidized methionine and acetylated protein N-termini were used. Additionally, Lys-6 for the spike-in internal standard was set as a label in the group-specific parameter section. A false discovery rate of 1% was used for peptides and proteins. A minimum peptide length of 6 amino acids was used. Razor and unique peptides were used for identification and quantification. Protein ratio values were reconstructed using median peptide ratio values across all three biological replicates for each experimental group where the final ratio for each protein was calculated by determining the ratio-of-ratio (PANTG/ Internal Standard/(WT/Internal Standard). Final ratios were input into the Perseus processing suite (Perseus version 1.2.0.13). Statistical analysis was performed using the Significance A outlier test where statistical significance based on magnitude fold-change was established at $P < 0.05$. Ratio values and Uniprot Protein identification numbers of differentially expressed proteins were uploaded to Ingenuity Pathway Analysis (IPA) to determine canonical pathways, networks and upstream regulators in the liver affected by increased pancreas-secreted PANDER. We note that the outlier test based on the ratio distribution of the combined replicates was performed to increase coverage depth of differentially expressed proteins. The limitation of this approach is the increased false discovery rate of differentially expressed proteins as variance within groups is not specifically considered in the statistical filtering. Given only lysine-terminated tryptic peptides were used for relative quantitation, coverage of quantifiable proteins was limited

(more so for lower abundance proteins) and therefore the Significance A filtering approach was utilized in order to enhance bioinformatic analysis. Additionally, we have generated a modified ProteinGroups file generated by MaxQuant that lists relative expression ratios for each biological replicate, showing all proteins with measurable relative standard deviation (RSD) values. In order to achieve statistical significance based on 1.5-fold change in expression (relative to wild-type, which is a value close to the Significance A test cut-off for significance at $p<0.05$ for the three metabolic conditions) using the Student's t-test (with the assumption that variance is the same at higher expression), approximately 30% RSD or less would be needed. For higher fold-change values (>2-fold), statistical significance using the Student's t-test could be achieved at RSD values measured for most proteins in the modified ProteinGroups file. The modified protein list represents all hepatic proteins that are quantifiable with the methodology and instrumentation used in this study. This file as well as all mass spectrometric data have been deposited to the ProteomeXchange Consortium via the PRIDE partner repository with the dataset identifier PXD004171 and 10.6019/PXD004171. In addition, further raw data and a detailed description of the proteomic analysis can be found in the *Data in Brief* manuscript associated with this study including Venn-Diagrams of unique proteins across metabolic states (Fig. 1, *Data in Brief* article) and complete listing of all differentially expressed proteins (Supplementary Tables 1–3, *Data in Brief* article) (Athanason, 2016).

2.6. Immunoblotting

Approximately 100 mg of tissue was excised from a lobe of mouse liver for tissue lysis. Liver samples were identical from those obtained during the SILAC analysis as detailed earlier. In brief, following isolation the liver was submerged in cold T-PER lysis buffer (Thermo) supplemented with 1X HALT protease inhibitor and lysed using a Qiagen TissueRupter until tissue debris was no longer visible. Cellular lysate was then heated at 95°C for five minutes followed by brief sonication. The tissue lysate was cleared by centrifugation at 16000× *g* for 5 min and the supernatant was collected and stored at −80°C prior to further analysis. Protein concentration was quantified using the Pierce BCA Protein assay following the manufacturer's protocol. Fifty μg was separated by SDS-PAGE (Mini-PROTEAN TGX Pre-Cast gels, 4–20%) and electro-transferred to a PVDF membrane using the iBlot semi-dry transfer apparatus (Invitrogen). PVDF membranes were then probed with primary antibodies against FAS, (C20G5, Cell Signaling Technology), LXRα (P-20, Santa Cruz), and CYP7A1 (ab65596, Abcam). All primary antibodies were diluted 1:500 in StartBlock Blocking Buffer (Thermo). Detection was achieved utilizing horseradish-peroxidase-conjugated goat secondary antibody (Bio-Rad) diluted 1:10,000 in StartBlock followed by chemiluminescence detection using Pierce ECL Western Blotting Substrate (Thermo). Emitted signal was detected using the Amersham™ Imager 600 (GE Healthcare Life Sciences). Relative protein levels were normalized to GAPDH (2118, Cell Signaling) and expression levels and densitometry analysis were quantified with ImageQuantTL (GE Healthcare Life Sciences).

2.7. Cell culture and transient transfections

BNL-CL2 (BALB/c embryonic normal liver) cells were cultured until passage five in standard DMEM (4.5g/L glucose, L-glutamine and sodium pyruvate) supplemented with

10% FBS and 1% PenStrep (Thermo) at 37 °C, 5% CO_2. Approximately 2×10^5 cells per well were plated in a tissue culture treated 24-well dish (Becton-Dickinson). After 24 hours, media was replaced with DMEM without glucose, L-glutamine and sodium pyruvate supplemented with 1% FBS for 4 hours prior to transfection. LXRα signaling plasmids and control plasmids (Cignal Reporter Assay Kit, Qiagen) were transfected using Lipofectamine 2000 (Invitrogen, Carlsbad, CA). Transfection of each plasmid was performed in triplicate in two independent experiments. Two hours post transfection, media was replaced with DMEM supplemented with 1% FBS and 1% PenStrep with the addition of PANDER (0.25 nM, 0.5 nM and 1nM) for 18 hours. Cells were washed with PBS and lysed in 100 μl of 1X Glo Lysis Buffer (Promega), utilizing the Dual-Luciferase Reporter Assay System (Promega) for luciferase activation. Signal emission was detected with a Monolight 3010 luminometer (Analytical Luminescence Laboratory, San Diego, CA).

3. RESULTS

3.1 SILAC Proteomic characterization of PANTG liver reveals increased hepatic lipogenesis

To comprehensively examine the PANDER-induced hepatic proteome, we performed SILAC-based quantitative proteomics on our PANTG model. The PANTG is an ideal candidate for our investigation due to pancreatic-specific overexpression of PANDER resulting in robust increased circulating levels as compared to wild-type mice along with resultant impaired glucose tolerance, hepatic insulin resistance and increased hepatic triglyceride levels (Robert-Cooperman et al., 2014). Our quantitative proteomic approach was performed on the PANTG model in comparison to WT mice in the context of 3 metabolic conditions of fasting, fed and insulin-stimulated to examine the impact of PANDER across numerous metabolic states. Following exposure to the various metabolic conditions, livers from PANTG and age/gender matched WT mice were collected and subsequently processed by tryptic digestion, desalting and SCX chromatography followed by mass spectrometry as detailed in Figure 1. Across all metabolic conditions, MaxQuant identified a total of 19,423 unique peptides (Complete data files deposited to the ProteomeXchange Consortium via the PRIDE partner repository with the dataset identifier PXD004171 and 10.6019/PXD004171). Of those, there were 228, 239 and 189 significantly differently expressed and quantifiable proteins in the fasted, fed and insulin-stimulated conditions within the PANTG liver as compared to WT, respectively (Listed in Supplementary Table 1 and fully detailed in reference (Athanason, 2016). Based on proteomic examination by IPA of the differentially expressed proteins, the top predicted primary molecular and cellular functions altered in the PANTG for all metabolic states was lipid metabolism based on −log(p-value) score as determined using the Significance A outlier test (Fig. 2). Within the fasting, fed and insulin-stimulated conditions, 51, 42 and 50 differentially expressed proteins, respectively, with lipogenic associated functions were identified (Listed in Supplementary Table 2 and fully detailed in reference (Athanason, 2016). The most significant metabolic changes in the predicted activation state were found during insulin stimulation with numerous functions having a significant predicted activation as determined by z-score in IPA (z-score values >2 or <−2 indicate activation or inhibition, respectively). These functions included fatty acid synthesis, concentration of lipid, concentration of fatty acid, oxidation of lipid and conversion of lipid (Table 1). The most

significantly activated lipogenic that were identified included fatty acid synthesis and concentration of lipid with 27 proteins converging on these predicted activated networks (Figure 3).

Some of the most notable differentially expressed enzymes involved in lipogenesis included fatty acid synthase (FASN), ATP citrate lyase (ACLY), and sterol-CoA desaturase-1 (SCD) (Fig 3.).

3.2. Proteomic identification of PANDER-induced hepatic LXR pathway

Due to the significant change in hepatic lipogenesis as determined by our proteomic approach, a mechanism or canonical pathway was then evaluated to potentially identify the etiology supporting this phenotype. Therefore, IPA was used to identify putative canonical pathways in all metabolic states that could potentially regulate the observed lipogenic pathways. Network analysis revealed that Liver X Receptor activation was identified as the most significantly predicted overall affected pathway across metabolic states (Fig. 4). In addition, acute phase response signaling was also revealed as a significant canonical pathway.

3.3. Validation of PANDER-induced hepatic LXR pathway and fatty acid synthase expression

Liver X receptors (LXR) are transcription factors belonging to the class II nuclear receptor superfamily and are composed of 2 isoforms (Edwards, Kennedy and Mak, 2002, Steffensen and Gustafsson, 2004, Ducheix, Montagner, Theodorou et al., 2013). LXRα is highly expressed in the liver, intestine, and adipose tissues whereas LXRβ is ubiquitously expressed. Upon activation, LXRs form a heterodimer with the retinoid X receptor α, which binds to LXR response elements and enhances targeted gene expression in a functional-dependent manner. LXRs appear to regulate overall glucose, cholesterol, bile acid, and triglyceride homeostasis (Baranowski, 2008). One of the most critical gene targets governed by LXR involved in lipogenesis is FASN, which was shown by our proteomic analysis to be significantly increased in PANTG livers in all metabolic states (Joseph, Laffitte, Patel et al., 2002, Talukdar and Hillgartner, 2006) (Supplementary Table 2). Several LXR targets including FASN and SCD1 not only pass the Significance A outlier test based on the ratio distribution of the combined biological replicates but also demonstrate statistical significance using the t-test ($p<0.05$) in the insulin-stimulated group. Other targets such as CYP7A1 and CD36 are lower abundance proteins with limited peptide coverage, which affect quantitation accuracy. Therefore, these proteins require further validation by a targeted approach such as western blot analysis. We then sought to precisely examine expression of LXR and dominant targets of LXR such as FASN and CYP7A1 in the PANTG liver. Livers obtained during the proteomic investigation of PANTG were also examined for levels of LXRα expression. In brief, PANTG and WT livers obtained and snap-frozen as previously detailed for the proteomic analysis were probed for LXRα, FASN and CYP7A1 expression by western analysis. Samples from the insulin-stimulated conditions were examined since this metabolic condition demonstrated the most significant differentially expressed lipid metabolism network (Fig. 2). During insulin-stimulated conditions, LXRα was significantly increased (*Image J*, $P<0.05$) as compared to WT liver expression (Fig. 5). Levels of LXRβ

were similar between PANTG and WT (*data not shown*). In addition, hepatic expression of FASN and CYP7A1 were increased during insulin-stimulated conditions (*Image J*, $P<0.05$). In summary, LXRα and critical LXRα targets such as FASN and CYP7A1 were increased in PANTG model and indicates this pathway may potentially be activated during conditions of high circulating PANDER.

3.4. PANDER stimulates LXR transcriptional activity in-vitro

The above studies examined the abundance of LXR and targets of LXR in the PANTG liver. However, we will also wanted to determine if PANDER may govern or induce LXR transcriptional activity. To examine this, reporter gene analysis was performed using a commercially available LXR response element (LXRE) mediated luciferase assay (Qiagen, Cignal LXR Reporter Kit). This LXRα reporter assay measures the transcriptional activity of liver X receptor (LXR) and this was determined in the context of exogenous PANDER application. A liver derived cell line, BNL-CL2, was exposed to increasing concentrations of purified secreted PANDER (AstraZeneca) and LXR-directed transcriptional activity was measured. PANDER can significantly increase LXRE directed luciferase expression at a range of concentrations from 0.25 to 1 nM in a dose-dependent manner (Figure 6). Therefore, as matched with increased LXR expression in the liver of the PANTG, PANDER is also capable of directly stimulating LXR-directed transcriptional activity *in-vitro*.

4. DISCUSSION

This proteomic examination of the PANTG provided important mechanistic insight pertaining to the putative mechanism impacting lipid metabolism in the liver of mice with increased circulating PANDER sourced from the endocrine pancreas. Additionally, we demonstrated the strong utility for the implementation of quantitative mass spectrometry based proteomics for the investigation of metabolic disorders or the characterization of novel hormones regulating intracellular signaling. Evidence to date has demonstrated that PANDER can promote a selective hepatic insulin resistant (SHIR) phenotype whereby insulin signaling is partially inhibited and therefore hepatic glucose production and lipogenesis is increased (Robert-Cooperman et al., 2014), phenomena observed in T2D animal models and clinical human observations (Brown and Goldstein, 2008). Earlier studies demonstrated that PANDER overexpression induces fasting hyperglycemia by upregulating gluconeogenic gene pathways and subsequently increasing hepatic glucose output in mice (Robert-Cooperman et al., 2014, Li et al., 2011, Wilson, Schupp, Burkhardt et al., 2010). These effects were attributed to the presence of increased transcript levels of PEPCK and Glucose 6-phosphatase (G6Pase) due to inhibited phosphorylation of critical insulin signaling molecules such as Akt and AMPK. However, these similar studies revealed increased hepatic lipogenesis despite suppressed insulin signaling. Therefore, due to the complex nature of this metabolic process, we employed a comprehensive proteomic approach to identify putative novel mechanisms of this process. Our MS based methods demonstrated a proteomic profile similar to the observed lipogenic phenotype and supports the utility of using this tool to unravel complex signaling mechanisms.

With the creation of our pancreas-specific overexpressing mouse model, we have recently reported that the PANTG mice display fasting hyperglycemia attributed to impaired hepatic insulin sensitivity when circulating PANDER is overexpressed. A similar proteomic approach in the PANTG revealed upregulation of PEPCK and indicated a mechanism of PANDER-induced gluconeogenesis (Robert-Cooperman et al., 2014). This approach was limited though since our previous SILAC analysis employed ethanol treated AML-12 cells (murine hepatic cell line) to serve as the control “spike-in” internal standard for the liver and utilized for protein comparison. In addition, the prior proteomic examination was performed during a random re-fed uncontrolled metabolic state. This experimental design was certainly not ideal for making important comparisons during metabolic states and examining changes in the hepatic proteome. Therefore, our current approach employed controlled metabolic states (fasting, controlled fed, and insulin-stimulated) with a SILAC-labeled C57BL/6J murine liver (not AML-12 cell line) and evaluated in the established PANTG model. In our current study, we utilized a metabolically labeled “SILAC” mouse liver to provide a superior internal standard enhancing the capability to capture differences in the PANTG liver proteome as compared to the WT control.

Our proteomic data strongly complements the described published studies on PANDER’s role in the mouse liver with regard to inducing increased hepatic lipogenesis which has long been attributed to hyperinsulinemia (Assimacopoulos-Jeannet, Brichard, Rencurel et al., 1995), a hallmark of T2D and non-alcoholic fatty liver disease (Wanless and Lentz, 1990, Group, 1979). However, pertaining to lipid metabolism in the PANTG liver, little is known of the biochemistry generating the increase of lipid production, especially fatty acid synthesis and lipogenesis. In our study we have provided data indicating that PANDER overexpression acts to increase gene expression modulated by a similar nuclear binding protein: the liver X receptor (LXR). Insulin mediated activation of lipogenic pathways has been described extensively. LXR has been shown to drive overexpression of lipogenic genes in hyperinsulinemia conditions (Yoshikawa, Shimano, Amemiya-Kudo et al., 2001, Chen, Liang, Ou et al., 2004). Since the most significant effects of PANDER were observed during insulin-stimulatory conditions, our data suggests that PANDER acts in concert with insulin to potentially promote hepatic lipid production and fatty acid synthesis. Given the fact that PANDER does appear to be located within pancreatic β-cell insulin granules (Xu et al., 2005, Cao, Gao, Robert et al., 2003), this co-packaging may indicate complementary functionality in terms of distal biological effects on target tissues such as the liver. Increased hepatic lipid metabolism was also observed by proteomic analysis during fasting and fed conditions but not to the same level of statistical significance as insulin-stimulated. There are several potential putative mechanisms describing this effect. As mentioned previously, increased lipogenic gene regulation by PPARγ regulation has been described by blunted FOXO1 signaling (Li et al., 2011). Interestingly, our network analysis also indicated that PPARγ was a significantly predicted upstream regulator of the observed lipogenic effect in our PANTG model (data not shown). Alternatively, recent studies have indicated that Carbohydrate-Responsive Element Binding Protein (ChREBP) binds directly to the PANDER promoter (Ratliff, Athanason, Chechele et al., 2015). This gene plays a key role in the control of lipogenesis through the regulation of lipogenic genes (Dentin, Benhamed, Hainault et al., 2006, Iizuka, 2013). PANDER may be acting in concert with ChREBP

enhancing PANDER-induced lipogenesis (Ratliff et al., 2015). Our current data suggests a novel putative mechanism that implicates LXR as a key modulator of genes driving a hepatic steatotic phenotype in the PANTG mice. In the insulin-stimulated condition we saw this effect exaggerated where downstream targets of LXR such as FASN, ACC, SCD1, CYP7A1 and CD36 are all upregulated. Additionally, LDL was increased in the PANTG liver suggesting an increase of intercellular oxysterols. Oxysterol is the main activating ligand required for LXR-RXR dimerization (Janowski, Willy, Devi et al., 1996). LDL influx is mediated by certain cell membrane transporters, CD36 being one of them (Calvo, Gómez-Coronado, Suárez et al., 1998), leading to an increase in intracellular cholesterol content that can be subsequently oxidized (Noguchi, Numano, Kaneda et al., 1998). Taken together, we have demonstrated and validated that the LXR signaling pathway may be involved in PANDER-induced hepatic lipogenesis.

As detailed in prior review articles, PANDER has widespread interactions with both the liver and the endocrine pancreas (Wilson et al., 2011, Wang et al., 2012, Yang and Guan, 2013). Pancreatic islets obtained from the PANDER knockout mouse (PANDER KO) displayed an impaired glucose stimulated insulin secretion (GSIS) (Robert-Cooperman et al., 2010). The mechanism for this decreased biological function has yet to be determined precisely, although the observed inhibited intracellular Ca^{2+} response is believed to have a role in the impaired GSIS of the PANKO model. Importantly, LXR activation has been demonstrated to stimulate insulin secretion upon T0901317 (agonist of LXR) activation and promoting expression of FASN and ACC (also increased in our PANTG) in pancreatic islets (Efanov, Sewing, Bokvist et al., 2004, Efanov, Sewing, Bokvist et al., 2004). Concordantly, pancreatic islets from LXR knockout mice have disrupted GSIS with increased lipid deposition (Gerin, Dolinsky, Shackman et al., 2005). Although not experimentally confirmed in the PANKO model, the absence of PANDER may have inhibited pancreatic LXR expression resulting in the observed impaired GSIS. Another highly relevant finding is that chronic LXR activation particularly under high glucose conditions promotes pancreatic β-cells apoptosis (Choe, Choi, Kim et al., 2007). An identical biological effect that was initially widely reported for PANDER (Cao et al., 2003). Some of the earliest investigations demonstrated that PANDER could induced apoptosis of pancreatic β-cells and cell lines in a time and dependent manner (Cao et al., 2005, Cao et al., 2003). Taken together, PANDER induced LXR activation may provide a central rationale for the observed pleiotropic actions of this novel hormone in both the liver and pancreas.

During preparation of this manuscript, the first report examining circulating PANDER is currently *in-press* and measured these levels in an Asian population (n=212, aged 40–65) with varying degrees of glucose intolerance and T2D (Cao, Yang, Lai et al., 2015). Cao *et al.* revealed systemic PANDER levels are significantly correlated with increased fasting blood glucose (FBG), triglycerides, and high-density lipoprotein cholesterol. Furthermore, logistic regression analysis showed circulating PANDER was associated with increased risk of IGT or T2D following cofounder adjustment. In general, they found that elevated plasma PANDER was significantly associated with numerous metabolic syndrome components, which is certainly consistent with our proteomic investigation and other animal model studies revealing increased lipogenesis or hepatic steatosis during conditions of increased PANDER expression. Further studies are needed and the almost near absence of human

clinical and physiological *in-vivo* data presents a major limitation in the understanding of PANDER and etiological role within T2D. However, our proteomic investigation certainly supports the findings of this initial clinical study in that increased PANDER levels are associated with both increased hepatic lipogenesis and it's potential consequences in humans such as promoting or initiating T2D or Metabolic Syndrome. Given that LXR is an important gene in the regulation and homeostasis of cholesterol (Repa and Mangelsdorf, 2000), PANDER-induced effects on cholesterol may also be mediated by the LXR pathway. LXR also regulates the transcription of CYP7A1, the rate limiting step of converting cholesterol to bile acid as to effectively rid the cell of cholesterol (Chiang, Kimmel and Stroup, 2001). LXR activation also promotes the generation of other lipogenic genes increasing lipid accumulation and fatty acid synthesis. Accompanying this is the evidence of increased triglycerides seen phenotypically in the PANTG mouse in previous studies (Robert-Cooperman et al., 2014, Li et al., 2011). Additional studies are needed to precisely address both the molecular mechanism of PANDER-induced lipogenesis and the potential detrimental consequences when circulating levels are increased in humans in terms of the role in both initiation and onset of T2D or hepatic steatosis.

Supplementary Material

Refer to Web version on PubMed Central for supplementary material.

Acknowledgments

The authors would like to thank Dr. Lovisa Holmberg Schiavone from Reagents and Assay Development, Discovery Sciences, AstraZeneca for providing the murine secreted purified PANDER that was utilized in the *in-vitro* experiments. This work was supported by grants K01-DK070744 and R56-DK105173-01A1 (to B.R.B.) from the National Institute of Diabetes and Digestive and Kidney Diseases, National Institutes of Health.

References

1. Zhu Y, Xu G, Patel A, McLaughlin MM, Silverman C, Knecht K, Sweitzer S, Li X, McDonnell P, Mirabile R, Zimmerman D, Boyce R, Tierney LA, Hu E, Livi GP, Wolf B, Abdel-Meguid SS, Rose GD, Aurora R, Hensley P, Briggs M, Young PR. Cloning, expression, and initial characterization of a novel cytokine-like gene family. Genomics. 2002; 80:144–50. [PubMed: 12160727]
2. Burkhardt BR, Cook JR, Young RA, Wolf BA. PDX-1 interaction and regulation of the Pancreatic Derived Factor (PANDER, FAM3B) promoter. Biochim Biophys Acta. 2008; 1779:645–51. [PubMed: 18708173]
3. Burkhardt BR, Greene SR, White P, Wong RK, Brestelli JE, Yang J, Robert CE, Brusko TM, Wasserfall CH, Wu J, Atkinson MA, Gao Z, Kaestner KH, Wolf BA. PANDER-induced cell-death genetic networks in islets reveal central role for caspase-3 and cyclin-dependent kinase inhibitor 1A (p21). Gene. 2006; 369:134–41. [PubMed: 16412588]
4. Cao X, Yang J, Burkhardt BR, Gao Z, Wong RK, Greene SR, Wu J, Wolf BA. Effects of overexpression of pancreatic derived factor (FAM3B) in isolated mouse islets and insulin-secreting betaTC3 cells. Am J Physiol Endocrinol Metab. 2005; 289:E543–50. [PubMed: 15928025]
5. Hou X, Wang O, Li Z, Mou H, Chen J, Deng B, Qian L, Liu X, Le Y. Upregulation of pancreatic derived factor (FAM3B) expression in pancreatic beta-cells by MCP-1 (CCL2). Mol Cell Endocrinol. 2011
6. Mou H, Li Z, Yao P, Zhuo S, Luan W, Deng B, Qian L, Yang M, Mei H, Le Y. Knockdown of FAM3B triggers cell apoptosis through p53-dependent pathway. Int J Biochem Cell Biol. 2013; 45:684–91. [PubMed: 23246487]

7. Robert CE, Wu J, Burkhardt Br, Wolf B. Transgenic mice overexpressing the novel islet specific cytokine, PANDER, exhibit glucose intolerance. Diabetes. 2005; 54:A400.
8. Robert-Cooperman CE, Carnegie JR, Wilson CG, Yang J, Cook JR, Wu J, Young RA, Wolf BA, Burkhardt BR. Targeted disruption of pancreatic-derived factor (PANDER, FAM3B) impairs pancreatic beta-cell function. Diabetes. 2010; 59:2209–18. [PubMed: 20566664]
9. Wang O, Cai K, Pang S, Wang T, Qi D, Zhu Q, Ni Z, Le Y. Mechanisms of glucose-induced expression of pancreatic-derived factor in pancreatic beta-cells. Endocrinology. 2008; 149:672–80. [PubMed: 17962352]
10. Xiang JN, Chen DL, Yang LY. Effect of PANDER in betaTC6-cell lipoapoptosis and the protective role of exendin-4. Biochem Biophys Res Commun. 2012
11. Xu W, Gao Z, Wu J, Wolf BA. Interferon-gamma-induced regulation of the pancreatic derived cytokine FAM3B in islets and insulin-secreting betaTC3 cells. Mol Cell Endocrinol. 2005; 240:74–81. [PubMed: 16006032]
12. Yang J, Gao Z, Robert CE, Burkhardt BR, Gaweska H, Wagner A, Wu J, Greene SR, Young RA, Wolf BA. Structure-function studies of PANDER, an islet specific cytokine inducing cell death of insulin-secreting beta cells. Biochemistry. 2005; 44:11342–52. [PubMed: 16114871]
13. Yang J, Robert CE, Burkhardt BR, Young RA, Wu J, Gao Z, Wolf BA. Mechanisms of glucose-induced secretion of pancreatic-derived factor (PANDER or FAM3B) in pancreatic beta-cells. Diabetes. 2005; 54:3217–28. [PubMed: 16249448]
14. Zhuang F, Guan Q, Gao L, Yu C, Tian L, Wang J, Fan Y, Du D, Zhao J. Levels of serum pancreatic derived factor (PANDER) and their correlations with islet beta cell function in newly diagnosed type 2 diabetic patients. Shandong Daxue Xuebao. 2011; 48:1–4.
15. Robert-Cooperman CE, Dougan GC, Moak SL, Athanason MG, Kuehl MN, Bell-Temin H, Stevens SM Jr, Burkhardt BR. PANDER transgenic mice display fasting hyperglycemia and hepatic insulin resistance. J Endocrinol. 2014; 220:219–31. [PubMed: 24468680]
16. Li J, Chi Y, Wang C, Wu J, Yang H, Zhang D, Zhu Y, Wang N, Yang J, Guan Y. Pancreatic-derived factor promotes lipogenesis in the mouse liver: role of the Forkhead box 1 signaling pathway. Hepatology. 2011; 53:1906–16. [PubMed: 21412813]
17. Yang J, Wang C, Li J, Burkhardt BR, Robert-Cooperman CE, Wilson C, Gao Z, Wolf BA. PANDER binds to the liver cell membrane and inhibits insulin signaling in HepG2 cells. FEBS Lett. 2009; 583:3009–15. [PubMed: 19683528]
18. Biddinger SB, Hernandez-Ono A, Rask-Madsen C, Haas JT, Aleman JO, Suzuki R, Scapa EF, Agarwal C, Carey MC, Stephanopoulos G, Cohen DE, King GL, Ginsberg HN, Kahn CR. Hepatic insulin resistance is sufficient to produce dyslipidemia and susceptibility to atherosclerosis. Cell Metab. 2008; 7:125–34. [PubMed: 18249172]
19. Brown MS, Goldstein JL. Selective versus total insulin resistance: a pathogenic paradox. Cell Metab. 2008; 7:95–6. [PubMed: 18249166]
20. Wilson CG, Robert-Cooperman CE, Burkhardt BR. PANcreatic-DERived factor: Novel hormone PANDERing to glucose regulation. FEBS Lett. 2011
21. Wang C, Burkhardt BR, Guan Y, Yang J. Role of pancreatic-derived factor in type 2 diabetes: evidence from pancreatic beta cells and liver. Nutr Rev. 2012; 70:100–6. [PubMed: 22300596]
22. Cao X, Yang C, Lai F, Hong Z, Lin H, Liu J, Li Y. Elevated circulating level of a cytokine, pancreatic-derived factor, is associated with metabolic syndrome components in a Chinese population. Journal of Diabetes Investigation. 2015
23. Bell-Temin H, Culver-Cochran AE, Chaput D, Carlson CM, Kuehl M, Burkhardt BR, Bickford PC, Liu B, Stevens SM Jr. Novel Molecular Insights into Classical and Alternative Activation States of Microglia as Revealed by Stable Isotope Labeling by Amino Acids in Cell Culture (SILAC)-based Proteomics. Mol Cell Proteomics. 2015; 14:3173–84. [PubMed: 26424600]
24. Athanason MG, Stevens SM, Burkhardt BR. Hepatic SILAC Proteomic Data from PANDER Transgenic Model Data in Brief. 2016 Submitted.
25. Edwards PA, Kennedy MA, Mak PA. LXRs; oxysterol-activated nuclear receptors that regulate genes controlling lipid homeostasis. Vascul Pharmacol. 2002; 38:249–56. [PubMed: 12449021]
26. Steffensen KR, Gustafsson JA. Putative metabolic effects of the liver X receptor (LXR). Diabetes. 2004; 53(Suppl 1):S36–42. [PubMed: 14749264]

27. Ducheix S, Montagner A, Theodorou V, Ferrier L, Guillou H. The liver X receptor: a master regulator of the gut-liver axis and a target for non alcoholic fatty liver disease. Biochem Pharmacol. 2013; 86:96–105. [PubMed: 23542537]
28. Baranowski M. Biological role of liver X receptors. J Physiol Pharmacol. 2008; 59(Suppl 7):31–55. [PubMed: 19258656]
29. Joseph SB, Laffitte BA, Patel PH, Watson MA, Matsukuma KE, Walczak R, Collins JL, Osborne TF, Tontonoz P. Direct and indirect mechanisms for regulation of fatty acid synthase gene expression by liver X receptors. J Biol Chem. 2002; 277:11019–25. [PubMed: 11790787]
30. Talukdar S, Hillgartner FB. The mechanism mediating the activation of acetyl-coenzyme A carboxylase-alpha gene transcription by the liver X receptor agonist T0-901317. J Lipid Res. 2006; 47:2451–61. [PubMed: 16931873]
31. Wilson CG, Schupp M, Burkhardt BR, Wu J, Young RA, Wolf BA. Liver-specific overexpression of pancreatic-derived factor (PANDER) induces fasting hyperglycemia in mice. Endocrinology. 2010; 151:5174–84. [PubMed: 20844005]
32. Assimacopoulos-Jeannet F, Brichard S, Rencurel F, Cusin I, Jeanrenaud B. In vivo effects of hyperinsulinemia on lipogenic enzymes and glucose transporter expression in rat liver and adipose tissues. Metabolism. 1995; 44:228–233. [PubMed: 7869920]
33. Wanless IR, Lentz JS. Fatty liver hepatitis (steatohepatitis) and obesity: An autopsy study with analysis of risk factors. Hepatology. 1990; 12:1106–1110. [PubMed: 2227807]
34. Group NDD. Classification and diagnosis of diabetes mellitus and other categories of glucose intolerance. Diabetes. 1979; 28:1039–1057. [PubMed: 510803]
35. Yoshikawa T, Shimano H, Amemiya-Kudo M, Yahagi N, Hasty AH, Matsuzaka T, Okazaki H, Tamura Y, Iizuka Y, Ohashi K. Identification of liver X receptor-retinoid X receptor as an activator of the sterol regulatory element-binding protein 1c gene promoter. Molecular and cellular biology. 2001; 21:2991–3000. [PubMed: 11287605]
36. Chen G, Liang G, Ou J, Goldstein JL, Brown MS. Central role for liver X receptor in insulin-mediated activation of Srebp-1c transcription and stimulation of fatty acid synthesis in liver. Proc Natl Acad Sci U S A. 2004; 101:11245–50. [PubMed: 15266058]
37. Cao X, Gao Z, Robert CE, Greene S, Xu G, Xu W, Bell E, Campbell D, Zhu Y, Young R, Trucco M, Markmann JF, Naji A, Wolf BA. Pancreatic-derived factor (FAM3B), a novel islet cytokine, induces apoptosis of insulin-secreting beta-cells. Diabetes. 2003; 52:2296–303. [PubMed: 12941769]
38. Ratliff WA, Athanason MG, Chechele AC, Kuehl MN, Fernandez AM, MarElia CB, Burkhardt BR. Hepatic nutrient and hormonal regulation of the PANcreatic-DERived factor (PANDER) promoter. Molecular and Cellular Endocrinology. 2015; 413:101–112. [PubMed: 26123584]
39. Dentin R, Benhamed F, Hainault I, Fauveau V, Foufelle F, Dyck JR, Girard J, Postic C. Liver-specific inhibition of ChREBP improves hepatic steatosis and insulin resistance in ob/ob mice. Diabetes. 2006; 55:2159–2170. [PubMed: 16873678]
40. Iizuka K. Recent progress on the role of ChREBP in glucose and lipid metabolism. Endocrine Journal. 2013; 60:543–555. [PubMed: 23604004]
41. Janowski BA, Willy PJ, Devi TR, Falck J, Mangelsdorf DJ. An oxysterol signalling pathway mediated by the nuclear receptor LXRα. 1996
42. Calvo D, Gómez-Coronado D, Suárez Y, Lasunción MA, Vega MA. Human CD36 is a high affinity receptor for the native lipoproteins HDL, LDL, and VLDL. Journal of lipid research. 1998; 39:777–788. [PubMed: 9555943]
43. Noguchi N, Numano R, Kaneda H, Niki E. Oxidation of lipids in low density lipoprotein particles. Free radical research. 1998; 29:43–52. [PubMed: 9733021]
44. Yang J, Guan Y. Family with sequence similarity 3 gene family and nonalcoholic fatty liver disease. J Gastroenterol Hepatol. 2013; 28(Suppl 1):105–11. [PubMed: 23855304]
45. Efanov A, Sewing S, Bokvist K, Gromada J. Liver X receptor activation modulates insulin secretion in pancreatic beta-cells. Diabetologia. 2004; 47:A172–A172.
46. Efanov AM, Sewing S, Bokvist K, Gromada J. Liver X receptor activation stimulates insulin secretion via modulation of glucose and lipid metabolism in pancreatic beta-cells. Diabetes. 2004; 53:S75–S78. [PubMed: 15561926]

47. Gerin I, Dolinsky VW, Shackman JG, Kennedy RT, Chiang SH, Burant CF, Steffensen KR, Gustafsson JA, MacDougald OA. LXR beta is required for adipocyte growth, glucose homeostasis, and beta cell function. Journal of Biological Chemistry. 2005; 280:23024–23031. [PubMed: 15831500]

48. Choe SS, Choi AH, Kim KH, Chung JJ, Park JY, Lee JW, Lee KM, Lee IK, Kim JB. Chronic activation of liver X receptor induces beta-cell apoptosis through hyperactivation of lipogenesis. Diabetes. 2007; 56:A409–A409.

49. Cao X, Yang C, Lai F, Hong Z, Lin H, Liu J, Li Y. Elevated circulating level of a cytokine, pancreatic-derived factor, is associated with metabolic syndrome components in a Chinese population. J Diabetes Investig. 2015

50. Repa JJ, Mangelsdorf DJ. The role of orphan nuclear receptors in the regulation of cholesterol homeostasis. Annual review of cell and developmental biology. 2000; 16:459–481.

51. Chiang JY, Kimmel R, Stroup D. Regulation of cholesterol 7α-hydroxylase gene (CYP7A1) transcription by the liver orphan receptor (LXRα). Gene. 2001; 262:257–265. [PubMed: 11179691]

Highlights

- Hepatic SILAC proteomics was performed on PANDER transgenic
- 3304 total unique hepatic proteins were identified
- Cellular function altered in PANTG for all metabolic states was lipid metabolism
- Liver-X receptor activation predicted by proteomics and validated *in-vivo* and *in-vitro*
- Liver-X receptor activation may regulate the pleiotropic actions of PANDER

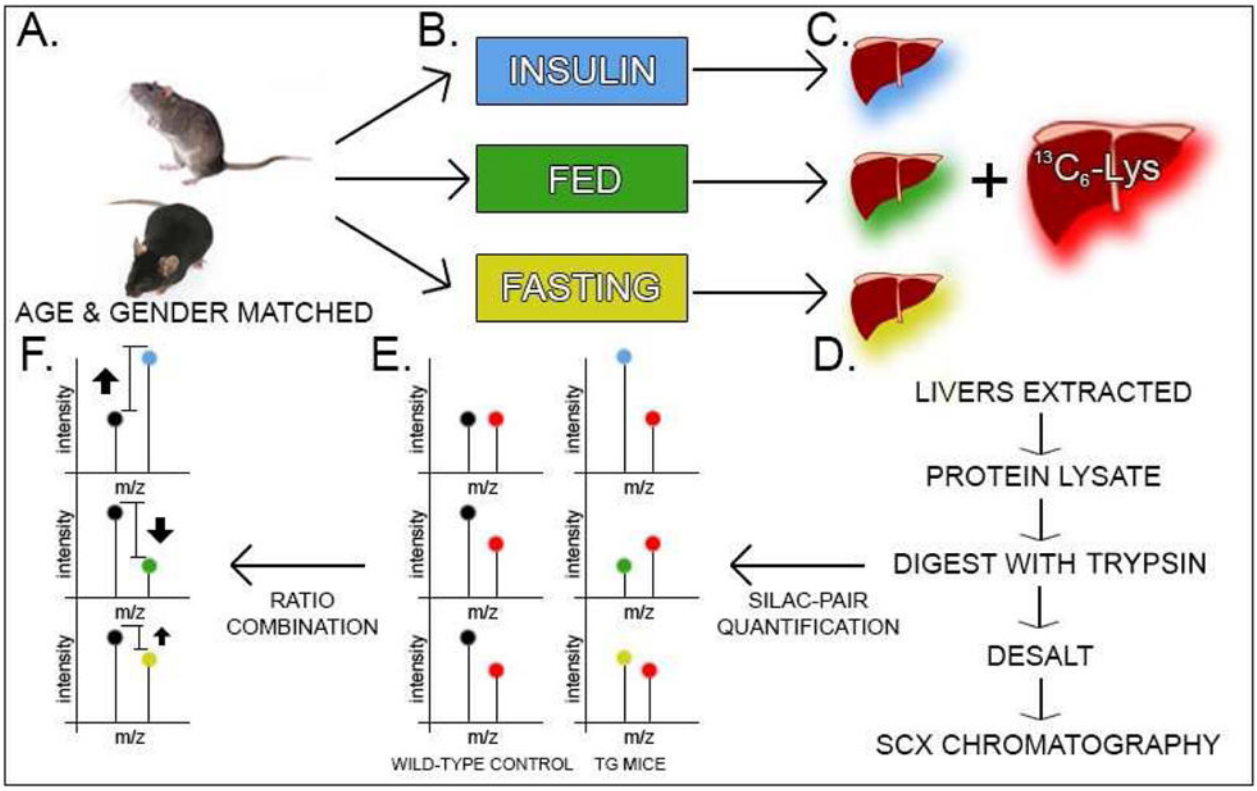

Figure 1. SILAC proteomic experimental approach for investigation of PANTG

A & B. Age and gender matched PANTG and WT mice at six weeks of age (N=3 per condition) were exposed to three metabolic states prior to liver extraction: fed, fasted and insulin-stimulated. Livers were immediately extracted following exposure to described metabolic conditions, snap-frozen and stored at −80°C. C. & D. 40 mg of liver tissue were lysed in cold lysis buffer (100mM Tris-HCl, 100mM DTT, 4% SDS and 1x HALT protease inhibitor) prior to heating at 95°C for five minutes followed by brief sonication. Identical process was performed on lives obtained from metabolically labeled “SILAC” mice (Cambridge Isotopes). The “heavy” protein lysate was combined with each experimental mouse liver protein lysate prior to tryptic digestion utilizing the FASP (Expedeon) method. Samples were desalted using solid phase enrichment C18 columns (The Nest Group, Inc.). Prior to LC-MS/MS, sample complexity was reduced by strong cation exchange chromatography. E. & F. Each biological sample was analyzed by tandem mass spectrometry. Normalized ratios from MaxQuant for each biological sample were inputted into the Perseus processing suite to determine statistical significance of quantitation values using a student’s two-tailed t test ($p < 0.05$) yielding 231 proteins in the fed condition, 246 proteins in the fasted condition and 191 proteins in the insulin-stimulated condition. Geometric means and Uniprot Protein Identification numbers were uploaded to Ingenuity Pathway Analysis (IPA) for canonical pathway and network analysis altered in the liver of mice with increased circulating PANDER.

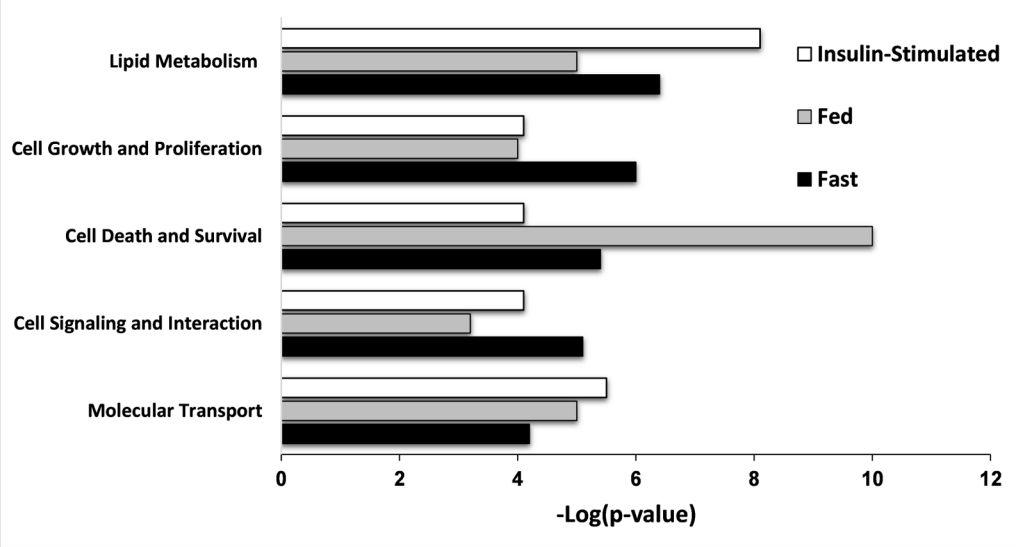

Figure 2. IPA determination of altered molecular and cellular functions with the PANTG liver

Molecular and cellular function analysis was determined based on the identified differentially expressed proteins of the PANTG and WT liver expression. Only functions that were identified in all metabolic states of insulin-stimulated *(Top Bar, White Fill)*, fed *(Middle Bar, Gray Fill)* and fasting *(Bottom Bar, Black Fill)* conditions with a score cutoff of −log(p-value) greater than two are shown as determined by Fisher's Exact test.

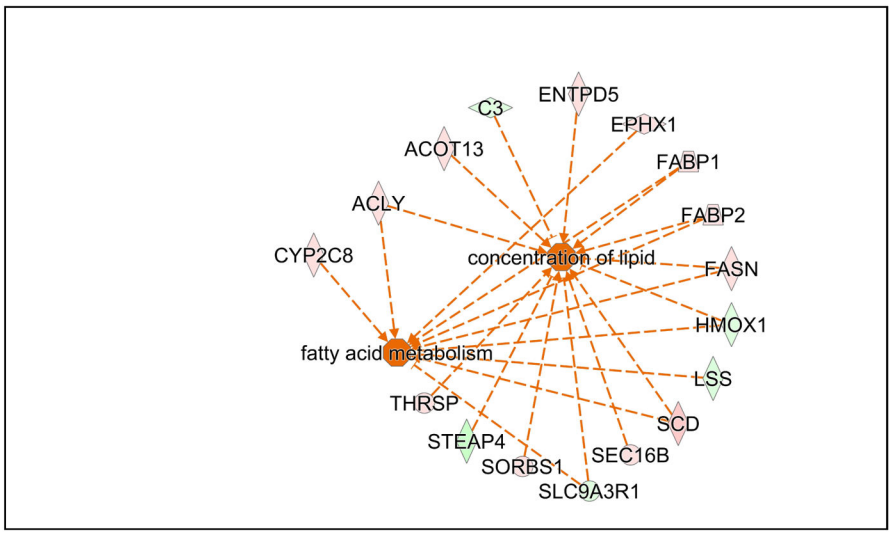

Figure 3. Network analysis of significantly differentially expressed lipogenic associated proteins during insulin stimulatory conditions in PANTG liver

Proteins with a positive association with increased lipogenic states of both fatty acid metabolism and concentration of lipid are shown. Orange dotted lines indicate strong direct association between shown proteins and the predicted activation of fatty acid metabolism and concentration of lipid. The outer nodes represent differentially expressed proteins where red and green represent up- and downregulation, respectively. Protein names are as follows, CYP2C8- cytochrome P450, family 2, subfamily C, polypeptide 8, ACLY- ATP citrate lyase, ACOT13- acyl-CoA thioesterase 13, C3- complement component 3, ENTPD5- ectonucleoside triphosphate diphosphohydrolase 5, EPHX1- epoxide hydrolase 1, FABP1 fatty acid binding protein 1, FABP2- fatty acid binding protein 2, FASN- fatty acid synthase, HMOX1- heme oxygenase 1, LSS- lanosterol synthase, SCD- stearoyl-CoA desaturase, SEC16B- SEC16 homolog B, endoplasmic reticulum export factor, SLC9A3R1- solute carrier family 9, subfamily A (NHE3, cation proton antiporter 3), member 3 regulator 1, SORBS1- sorbin and SH3 domain containing 1, STEAP4- STEAP family member 4, and THRSP- thyroid hormone responsive.

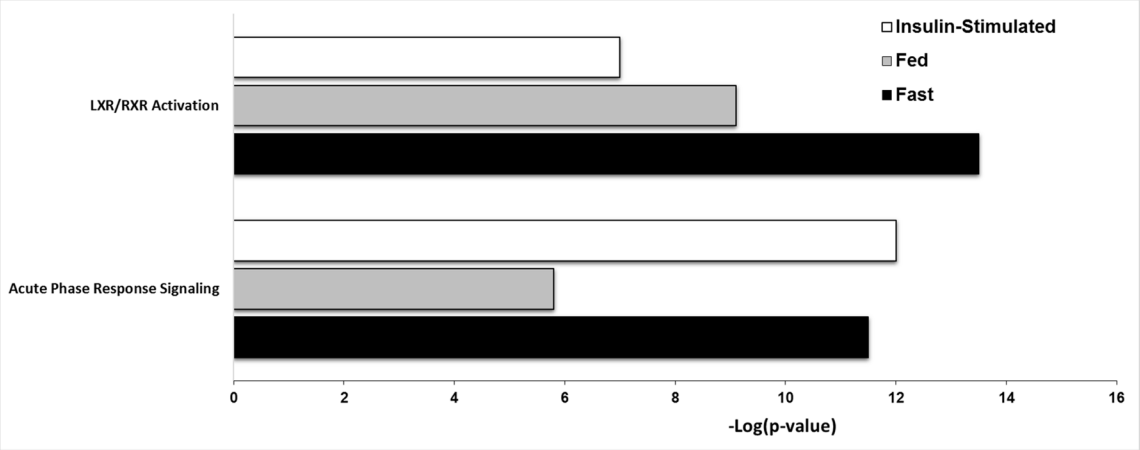

Figure 4. Canonical pathway analysis of significantly differentially expressed proteins during all metabolic conditions in PANTG liver

Canonical pathways with a score cutoff of −log(p-value) greater than 5 as determined by Fisher's Exact test and z-score greater than 2 are shown in metabolic states of insulin-stimulated *(Top Bar, White Fill)*, fed *(Middle Bar, Gray Fill)* and fasting *(Bottom Bar, Black Fill).*

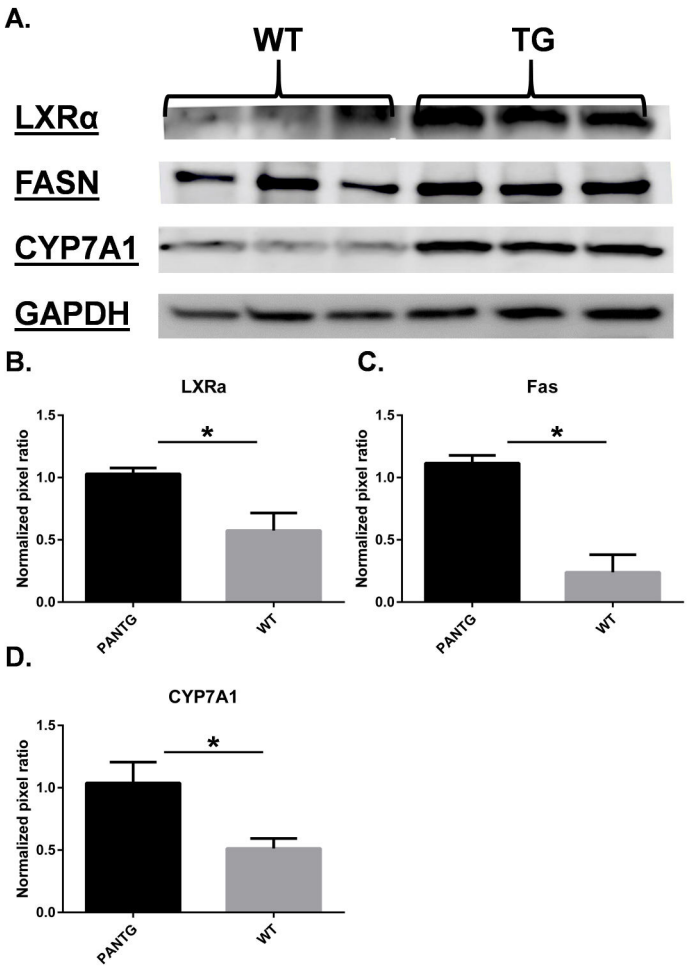

Figure 5. Western blotting and validation of LXRα and LXR targets (FASN and CYP7A1) in insulin-stimulated PANTG mice

(A) Liver lysate (40 μg) from age and gender matched PANTG mice during overnight fasting and insulin-stimulated conditions (n=3). Immunoblotting was performed to measure expression of LXRα, FASN, CYP7A1 and loading control of GAPDH. Lanes: 1–3 and 4–6 are WT and TG liver lysate, respectively. Densitometric analysis on (B) LXRα expression; (C) FASN and (D) CYP7A1. * $P < 0.05$ (ImageJ) for both conditions.

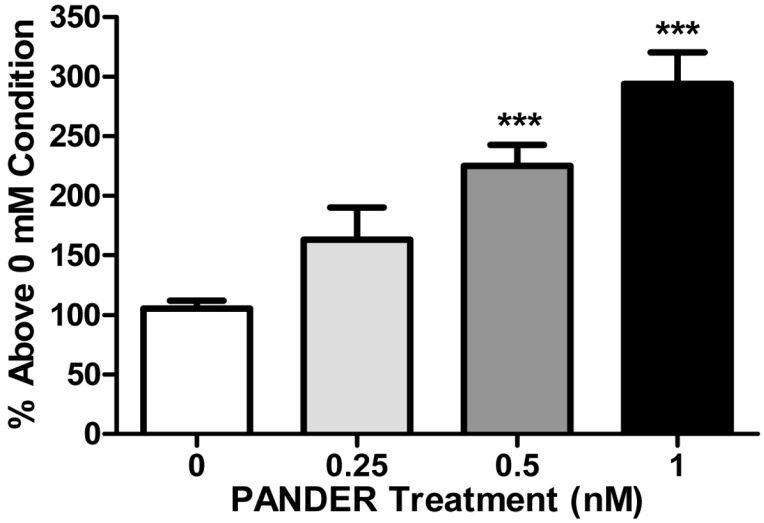

Figure 6. PANDER increased LXRE transcriptional activity in BNL-CL2 cells

Reporter gene analysis was performed on BNL-CL2 liver-derived cells transfected with LXRE-luciferase plasmids exposed to increasing concentrations of purified secreted PANDER (AstraZeneca) followed by measurement of luciferase activity. Treatments performed in triplicate in duplicate biological experiments. *** denotes $P < 0.001$ as determined by Students *t*-test from 0 nM PANDER condition.

Table 1

List of metabolic functions with significantly predicted increased activation state based on activation z-score identified during insulin conditions within PANTG liver as compared to WT.

Metabolic Functions	Predicted Activation State	Activation z-score	Total Proteins
fatty acid synthesis	Increased	2.9	27
concentration of lipid	Increased	2.57	26
oxidation of lipid	Increased	2.58	14
concentration of fatty acid	Increased	2.42	13
conversion of lipid	Increased	2.77	9